An unknown input observer approach to icing detection for unmanned aerial vehicles with linearized longitudinal motion

Andrea Cristofaro and Tor Arne Johansen

***Abstract*— The accretion of ice layers on wings and control surfaces modifies the shape of the aircraft and, consequently, alters performance and controllability of the vehicle. In this paper we propose an Unknown Input Observers framework to design icing diagnosis filters. A case-study is provided as support and validation of theoretical results.**

I. INTRODUCTION

Mechanical systems are usually exposed to possible malfunctions or anomalies; these may either be caused by faults occurring in actuators, effectors, sensors and other system components, or be structural, i.e. related to some modification of the nominal system dynamics. The problem of fault detection/identification and fault tolerant control has been widely investigated in recent years [1]; one of the major challenges to be faced in this topic is the correct identification of the fault behavior, in order to apply accommodation policies with the aim of recovering system performances or, at least, ensuring safe operational conditions.

Among structural faults, icing is a major issue for unmanned aerial vehicles (UAVs). The phenomenon of ice accretion on aircraft wings and control surfaces is a well recognized problem in aerospace engineering: when ice layers build up, they increase energy consumption and induce a safety risk, with the worst case scenario that the aircraft crashes [2]. Large airplanes are commonly equipped with efficient anti-icing and de-icing devices; however, these are mostly unsuitable for small unmanned aircrafts, due to UAVs simple architecture and limited payload. Ice formations on aircraft surfaces during flight are typically caused by the impact of supercooled water droplets (SWD). When a water droplet is cooled, it does not freeze until it reaches very low temperatures; however, the droplets will instantly freeze in the case of interaction with external agents, like aircrafts, releasing their own latent and accreting ice [3]. Both rate and amount of ice depend on the shape of the surface, its roughness, traveling body speed, temperature and droplet size. Large SWD lead to the accretion of clear-ice, having a smooth and clear structure; it is usually characterized by horn-like formations on the wing leading edge [4] and it is the most dangerous type of icing. Rime ice, an opaque and rougher formation, is instead caused by the impact of small SWD.

The modified shape of the leading edge due to ice changes lift, drag and pitch moment characteristics of the wing. For instance, an airfoil subject to horn-like ice formations may result in a lift coefficient reduction up to 40%, while the drag may be increased as much as 200%. Both these effects, and increased mass, require more engine power and implies a premature airfoil stall angle. An overview of the effects induced by icing is given in Figure 1.

Very recently some advanced de-icing devices for UAV have been proposed based on carbon nanotubes technology [5]; the wing surface can be painted with layers of coating material, which can be heated up very quickly using electricity. However, in order to guarantee the efficiency of the mechanism, it is very important to rely on icing detection schemes with fast and accurate responses. On the other hand, the availability of redundant control surfaces is a key advantage toward safe aircraft manoeuvring and stability in spite of icing. Control allocation [6] is a very helpful setup, as it allows to handle constraints and incorporate secondary objectives in a straightforward way. Moreover, several results on CA-based fault detection/isolation and fault tolerant control have been recently proposed [7] [8] [9] [10].

In this paper we present an unknown input observer based approach for icing detection in UAVs. In particular, referring to the longitudinal steady-state dynamics of the aircraft, we provide a design scheme for detection filters able to decouple icing effects from actuators or sensor faults. The proposed results are related to [11], where the lateral-directional dynamics is considered. The paper is structured as follows. The UAV model and the basic setup are given in Section II. Sections III and IV are dedicated to the design of icing detection filters possibly coping with actuators and sensor faults, respectively. Finally, a case-study is presented in Section V.

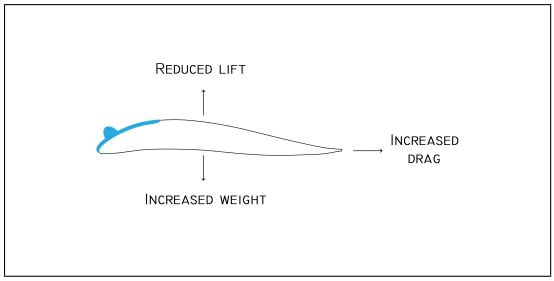

Fig. 1. Horn-like ice formation on airfoil: induced aerodynamical effects

A. Cristofaro and T.A. Johansen are with Center for Autonomous Marine Operations and Systems (AMOS) and with Department of Engineering Cybernetics, Norwegian University of Science and Technology , Norway. email: andrea.cristofaro@itk.ntnu.no, tor.arne.johansen@itk.ntnu.no

A. Cristofaro acknowledges funding support from ERCIM Alain Bensoussan Fellowship programme (ABCDE project - FP7 Marie Curie Actions)

This work is part of the work carried out at AMOS. It is supported by the Research Council of Norway through the Centres of Excellence funding scheme, project No. 223254 - AMOS.

II. MODEL AND SETUP

The longitudinal equations of motion of an aircraft are

$$\begin{cases} m(\dot{u}+qw-rv) = -mg\sin\theta - D\cos\alpha + L\sin\alpha + \mathcal{T} \\ \dot{q}I_{yy} - pr(I_{zz}-I_{xx}) + (p^2-r^2)I_{xz} = M_A + M_{\mathcal{T}} \\ m(\dot{w}+pv-qu) = mg\cos\theta - D\sin\alpha - L\cos\alpha \end{cases}$$

where (u, v, w) is the aircraft velocity relative to the wind, decomposed in the vehicle body coordinate system, θ is the pitch angle, (p, q, r) are, respectively, the roll, pitch and yaw rates; I_{ij} are the coefficients of the inertia matrix, m is the mass of the aircraft, α is the angle of attack, D is the drag coefficient, L is the lift coefficient, $\mathcal{T}$ is the thrust force and M_A, $M_{\mathcal{T}}$ are, respectively, the aerodynamical and thrust moments for the pitch. The above nonlinear model can be simplified by linearization with respect to some trim conditions; setting $c_\alpha := \cos\alpha_0$, the steady-state longitudinal linear dynamics is then given by [12]

$$\begin{bmatrix} \dot{\nu} \\ \dot{\alpha} \\ \dot{q} \\ \dot{\theta} \end{bmatrix} = \begin{bmatrix} X_\nu & X_\alpha c_\alpha & X_q & -g\cos\theta_0 \\ \frac{Z_\nu}{V_0 c_\alpha} & Z_\alpha & \frac{Z_q}{V_0 c_\alpha} & -\frac{g\sin\theta_0}{V_0 c_\alpha} \\ M_\nu & M_\alpha c_\alpha & M_q & 0 \\ 0 & 0 & 1 & 0 \end{bmatrix} \begin{bmatrix} \nu \\ \alpha \\ q \\ \theta \end{bmatrix}$$

$$+ \begin{bmatrix} X_{\delta_{th}} & X_{\delta_e} \\ 0 & \frac{Z_{\delta_e}}{V_0 c_\alpha} \\ M_{\delta_{th}} & M_{\delta_e} \\ 0 & 0 \end{bmatrix} \begin{bmatrix} \delta_{th} \\ \delta_e \end{bmatrix} = Ax + Bu.$$

The state variables x to be considered are the horizontal airspeed ν, the angle-of-attack α, the pitch rate q and the pitch angle θ. The symbols α_0, θ_0 and V_0 stand for some suitable trimmed values of angles and airspeed, respectively. The inputs u entering the system are the engine throttle δ_{th} and the elevator deflection δ_e. The nominal parameters entering the system matrices can be expressed as follows

$$X_\ell = \mu_{X_\ell}\bar{q}C_{X_\ell},\ Z_\ell = \mu_{Z_\ell}\bar{q}C_{Z_\ell},\ M_\ell = \frac{\mu_{M_\ell}\bar{q}C_{M_\ell}}{I_{yy}}$$

with $\ell \in \{\nu, \alpha, q, \delta_{th}, \delta_e\}$ and where $\bar{q} = 1/2\rho V_0^2$ is the trimmed dynamic pressure (being ρ the air density) and the factors μ_i depend on the wing spanned area $\mathcal{S}$ and on the elevator chord $\bar{c}$. The non-dimensional coefficients C_i are usually referred as stability and control derivatives relative to the trimmed values. The wind effect can be modeled as an additive disturbance vector $\mathcal{W}$ given by

$$\mathcal{W} = \begin{bmatrix} -\cos\theta_0 & -\sin\theta_0 \\ -\frac{\sin\theta_0}{V_0 c_\alpha} & \frac{\cos\theta_0}{V_0 c_\alpha} \\ 0 & 0 \\ 0 & 0 \end{bmatrix} \begin{bmatrix} \dot{\omega}_x \\ \dot{\omega}_z \end{bmatrix} = H_1\dot{\omega}_x + H_2\dot{\omega}_z,$$

where $\dot{\omega}_x$ and $\dot{\omega}_z$ are the wind accelerations in the horizontal and vertical direction, respectively. Assuming that the UAV is equipped with airspeed measurement device (pitot tube), compass, GPS and inertial sensors, all state variable are supposed to be available and hence the output matrix of the system verifies $C = I_{4\times 4}$.

Actuator faults may affect the system and these can be represented as an unknown input term $\mathcal{F}$ given by

$$\mathcal{F} = \begin{bmatrix} X_{\delta_{th}} & X_{\delta_e} \\ 0 & \frac{Z_{\delta_e}}{V_0 c_\alpha} \\ M_{\delta_{th}} & M_{\delta_e} \\ 0 & 0 \end{bmatrix} \begin{bmatrix} \varphi_{th} \\ \varphi_e \end{bmatrix} = B_1\varphi_{th} + B_2\varphi_e,$$

where φ_{th}, φ_e correspond to faults in propellers/engines and elevator, respectively.

The airspeed measurement devices, such as pitot tubes, may undergo possible faults too; moreover, recalling that the angle of attack α is not directly measured but it is computed through airspeed [13], it follows that also its estimation may be subject to errors in the case of sensor faults [14], [15]. We consider an additive model for airspeed sensor faults, i.e. we suppose the faulty output of the system to be given by

$$y = x + P\xi, \tag{1}$$

where

$$P = [\sigma_\nu\ \sigma_\alpha\ 0\ 0]^T \tag{2}$$

is a known vector and ξ is the fault severity factor.

Remark II.1 *Model (1) corresponds to increase the measured airspeed by an amount which depends on ice severity, as the blockage of pitot tubes leads to an increased pressure with a consequent over-estimation of relative velocity [16]. The vector P defined in (2) can be computed as follows. Let us assume that the measured airspeed components along x and z directions are given by*

$$\tilde{\nu}_x = \nu_x + \sigma_x\xi, \quad \tilde{\nu}_z = \nu_z + \sigma_z\xi$$

where ν_x, ν_z are the true airspeed values. and σ_x, σ_z are assumed to be known. By definition one has

$$y_1 = \tilde{\nu} := \tilde{\nu}_x, \quad y_2 = \tilde{\alpha} := \arcsin\frac{\tilde{\nu}_z}{\tilde{\nu}_x}.$$

Using first order Taylor expansions one gets

$$\tilde{\alpha} = \alpha + \frac{\nu_x\sigma_z - \nu_z\sigma_x}{\nu_x\sqrt{\nu_x^2 - \nu_z^2}}\xi + o(\xi);$$

choosing the trimmed values $\nu_{x,0},\ \nu_{z,0}$ according to $V_0 = \sqrt{\nu_{x,0}^2 + \nu_{z,0}^2}$ we can set

$$\sigma_\nu := \sigma_x$$
$$\sigma_\alpha := \frac{\nu_{x,0}\sigma_z - \nu_{z,0}\sigma_x}{\nu_{x,0}\sqrt{\nu_{x,0}^2 - \nu_{z,0}^2}}.$$

A. Icing effect model

The accretion of clear ice on the aircraft surfaces modifies the stability and control derivatives according to the following linear model [17]

$$C_i^\star = (1 + \eta K_i)C_i, \tag{3}$$

where η is the icing severity factor and the coefficient K_i depends on aircraft design and atmospheric conditions; the clean condition corresponds to $\eta = 0$, while the all

iced condition occurs for $\eta = 0.2$. It is worth noticing that the coefficients K_i turn out to be negative, so that model (3) corresponds to downscaling of control and stability derivatives.

As a consequence, the overall effect of icing can be modeled as an additive time-dependent disturbance term $\mathcal{E}\eta$, where η is a scalar unknown quantity and the vector $\mathcal{E}$ is assigned by

$$\mathcal{E} = \begin{bmatrix} K_{X_\nu} X_\nu & K_{X_{\alpha c_\alpha}} X_\alpha & K_{X_q} X_q \\ K_{Z_\nu} \frac{Z_\nu}{V_0 c_\alpha} & K_{Z_\alpha} Z_\alpha & K_{Z_q} \frac{Z_q}{V_0 c_\alpha} \\ K_{M_\nu} M_\nu & K_{M_\alpha} M_\alpha c_\alpha & K_{M_q} M_q \\ 0 & 0 & 0 \end{bmatrix} \begin{bmatrix} \nu \\ \alpha \\ q \end{bmatrix}$$

$$+ \begin{bmatrix} K_{X_{\delta_{th}}} X_{\delta_{th}} & K_{X_{\delta_e}} X_{\delta_e} \\ 0 & K_{Z_{\delta_e}} \frac{Z_{\delta_e}}{V_0 c_\alpha} \\ K_{M_{\delta_{th}}} M_{\delta_{th}} & K_{M_{\delta_e}} M_{\delta_e} \\ 0 & 0 \end{bmatrix} \begin{bmatrix} \delta_{th} \\ \delta_e \end{bmatrix}.$$

It is worth to note that icing may also alter the airspeed measurements, both directly and indirectly; in particular, ice formations inside the pitot tubes are not unlikely. The following block diagram illustrates all possible interactions of icing with the UAV system.

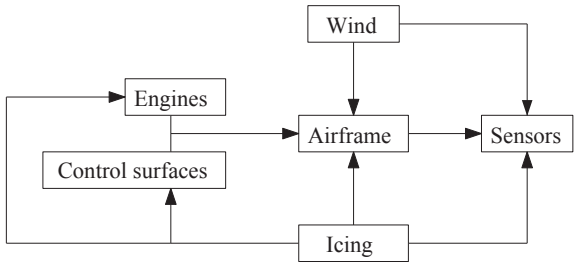

Fig. 2. Icing interaction with system components

B. Unknown inputs allocation

Allocation schemes are usually introduced in order to handle constraints and secondary objectives in systems with a redundant set of inputs. This is typically expressed through a low-level effector model

$$\tau = Gu,$$

with $k = dim(\tau) < dim(u) = m$, together with the high-level dynamics

$$\dot{x} = Ax + B\tau.$$

The allocation framework can also be adopted for studying the effects of redundant unknown inputs. In particular, one is interested in the identification of specific combinations of inputs entering the system, even if the magnitude of each single input is not directly available. To this end, we give the following definition.

Definition II.1 *Let $\ell = \mathrm{rank}\, G \leq k$. A set of ℓ linearly independent columns of G, namely $G_{i_1}, ...G_{i_\ell}$, is said a fundamental set of directions for the input allocation scheme.*

It is worth to note that, if $\hat{G}$ is the matrix formed by a fundamental set of directions, then, for any $\tau_c \in \mathrm{Im}G$, there exists a reduced-order input $\hat{u} = (u_{i_1}, ..., u_{i_\ell})$ satisfying the identity $\tau_c = \hat{G}\hat{u}$.

Referring to the considered UAV model, the overall effect of wind, actuator faults and icing is a vector of the form $[\tau\ 0]^T$, with $\tau \in \mathbb{R}^3$; this is generated by the "virtual" effector model

$$\tau = Gv,$$

where $v = [\dot{\omega}_x\ \dot{\omega}_z\ \phi_{th}\ \phi_e\ \nu\ \alpha\ q\ \delta_{th}\ \delta_e]^T$ and the matrix $G \in \mathbb{R}^{3\times 9}$ can be easily obtained from the expressions of the terms $\mathcal{W}, \mathcal{F}$ and $\mathcal{E}$[1].

Since $\mathrm{rank}G = 3$, several fundamental sets of directions can be considered; the proposed fault isolation approach is based on optimally selecting such sets of directions from the matrix G in order to design detection filters with a geometric separation property, i.e. able to assign characteristic output directions to wind disturbances, actuator or sensor faults and icing effects.

III. Actuator faults and icing diagnosis

Combining airspeed measurement with GPS measurement of the ground speed and inertial sensors, the horizontal wind component $\dot{\omega}_x$ can be estimated in a satisfactory way [18]. On the other hand, an estimation inaccuracy of wind force can be handled by the icing diagnosis algorithm introducing suitable detection thresholds, if the error size is comparable with other parameter uncertainties possibly affecting the model. For sake of clarity of presentation we do not consider explicitly such inaccuracy.

Assumption III.1 *The horizontal wind acceleration $\dot{\omega}_x$ is assumed to be known at each time instant.*

As a consequence, setting $x = [\nu, \alpha, q, \theta]$ and $u = [\delta_{th}, \delta_e, \dot{\omega}_x]$, the system can be rewritten in the compact form

$$\dot{x} = Ax + B_{ext}u + \mathcal{D}, \tag{4}$$

with $B_{ext} = [B \quad H_1]$ and where $\mathcal{D} = \mathcal{W}_z + \mathcal{F} + \mathcal{E}\eta$ is the overall uncertainty term, incorporating vertical wind, actuator

[1] The explicit expression of the matrix G is the following:

$$G = \begin{bmatrix} -\cos\theta_0 & -\sin\theta_0 & X_{\delta_{th}} & X_{\delta_e} & \eta K_{X_\nu} X_\nu & \eta K_{X_\alpha} X_\alpha & \eta K_{X_q} X_q & \eta K_{X_{\delta_{th}}} X_{\delta_{th}} & \eta K_{X_{\delta_e}} X_{\delta_e} \\ -\frac{\sin\theta_0}{V_0 c_\alpha} & \frac{\cos\theta_0}{V_0 c_\alpha} & 0 & \frac{Z_{\delta_e}}{V_0 c_\alpha} & \eta K_{Z_\nu} \frac{Z_\nu}{V_0 c_\alpha} & \eta K_{Z_\alpha} Z_\alpha & \eta K_{Z_q} \frac{Z_q}{V_0 c_\alpha} & 0 & \eta K_{Z_{\delta_e}} \frac{Z_{\delta_e}}{V_0 c_\alpha} \\ 0 & 0 & M_{\delta_{th}} & M_{\delta_e} & \eta K_{M_\nu} M_\nu & \eta K_{M_\alpha} M_\alpha c_\alpha & \eta K_{M_q} M_q & \eta K_{M_{\delta_{th}}} M_{\delta_{th}} & \eta K_{M_{\delta_e}} M_{\delta_e} \end{bmatrix}$$

faults and icing effects. Now by construction the vertical wind is assigned by

$$\mathcal{W}_z = H_2 \dot{\omega}_z,$$

while the actuator fault term is given by

$$\mathcal{F} = B_1 \phi_{th} + B_2 \phi_e.$$

Assumption III.2 *The vectors B_1, B_2 and H_2 are a fundamental set of directions, i.e.*

$$\text{rank}[B \quad H_2] = 3.$$

We recall now the classical definition of unknown input observers [19]: the main advantage of such observers is that, if some structural conditions are met, the parameters can be designed such that the resulting estimation error is independent of some inputs of the systems, even if these are not measured directly.

Definition III.1 *Consider the linear system*

$$\begin{cases} \dot{x}' = A'x' + B'u_0 + B'_{un}u'_{un} \\ \\ y' = C'x', \end{cases} \tag{5}$$

where the input u_{un} is supposed to be unknown, and define the full-order observer

$$\begin{cases} \dot{z}(t) = Fz(t) + RB'u_0(t) + Sy'(t) \\ \\ \hat{x}(t) = z(t) + Ty'(t) \end{cases} \tag{6}$$

Setting $S = S_1 + S_2$, if the following conditions are satisfied

$$R = I_{n\times n} - TC \tag{7}$$

$$F = RA' - S_1 C, \quad \sigma(F) \in \mathbb{C}^- \tag{8}$$

$$S_2 = FT, \tag{9}$$

then (6) is an unknown input observer for system (5) with estimation error $\epsilon_a(t) = x'(t) - \hat{x}(t)$ given by

$$\dot{\epsilon}_a = F\epsilon_a + RB'_{un}u_{un}.$$

The matrix S_1 is a gain parameter to be used for assigning the eigenvalues of F, while T has to be tuned in order to constrain the range of the matrix RB_{un}; we notice that the filter design requires the knowledge of the input matrix B'_{un}. The basic idea of the proposed approach is to set T in order to assign different output directions of residuals for wind effect, actuator faults and icing effects respectively, with the aim of identifying the true behavior of the system malfunctions. However, due to superposition of effects and lack of degrees of freedom in the observer design, the fault isolation cannot be achieved through a trivial scheme and some clever method is necessary.
To this purpose, we first notice that, by Definition II.1 and Assumption III.2, the following condition holds:

$$\mathcal{E} = \mathcal{E}(t) \in span[B \ H_2] \ \forall t \geq 0.$$

Let us denote by $\mathbf{e}_1, \mathbf{e}_2, \mathbf{e}_3, \mathbf{e}_4$ the basis vectors of the output space $\mathbb{R}^4$. Referring to system (4) with $B' = B_{ext}$, our target is to design an observer with the following property:

$$RB_1 = \mathbf{e}_1, \quad RB_2 = \mathbf{e}_2, \quad RH_2 = \mathbf{e}_3 \tag{10}$$

and

$$F\mathbf{e}_i = \lambda_i^F \mathbf{e}_i \ \forall i = 1, 2, 3. \tag{11}$$

Proposition III.1 *Setting $\bar{B}_A = [B_1 \ B_2 \ H_2]$, $I_3^{(4)} = [\mathbf{e}_1 \ \mathbf{e}_2 \ \mathbf{e}_3]$, and choosing $\lambda_i^F > 0$, T and S_1 according to*

$$T = (\bar{B}_A - I_3^{(4)})\bar{B}_A^{-L}, \quad S_1 = -diag(\lambda_1^F, ..., \lambda_4^F) + A - TA,$$

conditions (10)-(11) are satisfied.

Proof: The proof is straightforward observing that all state variables are measured, i.e. $C = I_{4\times 4}$. ■

Since the state of the system is completely known, without loss of generality one can assume $\epsilon_a(0) = 0$. As a consequence, the estimation error belongs to a linear subspace that is totally determined by the range of the matrix $R\bar{B}_A$. For sake of clarity in the presentation, let us introduce the following subspaces:

$$\mathcal{V}_i = span\{\mathbf{e}_i\}, \ \mathcal{V}_{i,j} = span\{\mathbf{e}_i, \mathbf{e}_j\}, \ \mathcal{V}_\sharp = span \, I_3^{(4)}, \tag{12}$$

with $i, j = 1, 2, 3$ and $i \neq j$. Based on the previous observer design, we can state the following decision algorithm addressing fault isolation.

Decision Algorithm 1.

$\epsilon_A(t) \neq 0 \Rightarrow$ `Alarm: unexpected effect`

```
if ϵ_A(t) ∈ V_1 then f_th ≠ 0:
  ''Fault in thrust ''
if ϵ_A(t) ∈ V_2 then f_e ≠ 0:
  ''Fault in elevator ''
if ϵ_A(t) ∈ V_3 then w_z ≠ 0:
  ''Vertical wind disturbance''
if ϵ_A(t) ∈ V_{1,2} then f_th · f_e ≠ 0:
  ''Faults in thrust and elevator''
if ϵ_A(t) ∈ V_{1,3} then f_th · w_z ≠ 0:
  ''Fault in thrust and wind disturbance''
if ϵ_A(t) ∈ V_{2,3} then f_e · w_z ≠ 0:
  ''Fault in elevator and wind disturbance''
if ϵ_A(t) ∈ V_♯ then f_th · f_e · w_z ≠ 0 or η ≠ 0:
  ''Possible icing''
```

Remark III.1 *It is worth to note that the last scenario $\epsilon(t) \in \mathcal{V}_\sharp$ can be generally interpreted as an icing detection condition without any ambiguity: as a matter of fact, icing typically causes changes on operational conditions of both control surfaces and engines.*

Remark III.2 *The speed of convergence of residuals can be tuned by means of the eigenvalues $\lambda_1^F, ..., \lambda_4^F$ in (11), that can be arbitrarily assigned. In the case of slowly-variant or*

uncertain parameters, some detection thresholds have to be introduced. Statistical methods, such as hypothesis testing, may be very helpful for choosing the proper thresholds and evaluating the corresponding time-windows.

IV. Sensor faults and icing diagnosis

We consider now the problem of decoupling structural icing effects from airspeed measurement faults. We will refer to identity (1) and we notice that, in the case of airspeed measurement malfunctions, the wind speed will be no longer correctly estimated. As the wind estimation may be performed by comparing airspeed measurements with GPS-based ground speed measurements, a linear model for such error can be considered according to the sensor fault model (1). Moreover, for sake of simplicity, we do not take into account the vertical wind component.

Assumption IV.1 *The measure of horizontal wind acceleration component $\dot{\omega}_x$ is affected by a fault-dependent error $c_\omega \xi$, where the coefficient c_ω is supposed to be known.*

Assumption IV.2 *The vertical wind acceleration component $\dot{\omega}_z$ is assumed to be negligible, i.e. $\dot{\omega}_z \simeq 0$.*

Consider the UIO defined by (6)-(9) and set the estimation error

$$\epsilon_s = y - \hat{x} = x + P\xi - \hat{x}.$$

Based on the definition of $\hat{x}$, straightforward computations yield the following expression for the error dynamics

$$\dot{\epsilon}_s = F\epsilon_s + R\mathcal{E} + R(c_w H_1 + AP)\xi + RP\dot{\xi}.$$

Setting $H_P := c_w H_1 + AP$, the above expression reduces to

$$\dot{\epsilon}_s = F\epsilon_s + R\mathcal{E} + RH_P\xi + RP\dot{\xi}$$

where, up to unlikely degenerate cases, one has $\mathcal{E} \notin span\{H_P, P\}$. Assuming, without loss of generality, that

$$\mathrm{rank}[H_P \ P] = 2,$$

let us select a vector $\mathbf{v}_P$ of the form $[\star \ \star \ 0]^T$ and such that $\{\mathbf{v}_P, H_P, P\}$ is a fundamental set of directions. We point out that, due to the presence of both ξ and its derivative $\dot{\xi}$, the isolation of sensor faults requires two independent output directions. In particular, we aim at designing the observer fulfilling

$$span\, R[H_P \ P] = \mathcal{V}_{1,2}, \quad R\mathbf{v}_P = \mathbf{e}_3, \tag{13}$$

together with

$$F\mathbf{e}_i = \lambda_i^F \mathbf{e}_i \ \forall i = 1, 2, 3. \tag{14}$$

Proposition IV.1 *Setting $\bar{B}_S = [H_P \ P \ \mathbf{v}_P]$, $I_3^{(4)} = [\mathbf{e}_1 \ \mathbf{e}_2 \ \mathbf{e}_3]$, and choosing T and S_1 according to*

$$T = (\bar{B}_S - I_3^{(4)})\bar{B}_S^{-L}, \quad S_1 = -diag(\lambda_1^F, ..., \lambda_4^F) + A - TA,$$

conditions (13) and (14) are satisfied.

The following simple diagnosis algorithm can be stated.

Decision Algorithm 2.

$\epsilon_s(t) \neq 0 \Rightarrow$ `Alarm: unexpected effect`

`if` $\epsilon_s(t) \in \mathcal{V}_{1,2}$ `then` $\xi \neq 0$:
  ``Fault in the airspeed sensor''

`if` $\epsilon_s(t) \in \mathcal{V}_\sharp$ `then` $\eta \neq 0$:
  ``Possible icing''

Remark IV.1 *In the case of slowly-varying sensor faults, i.e. $\dot{\xi} \simeq 0$, the above design technique can be readily adapted to face actuator and sensor faults at the same time. In particular, provided that the vectors B_1, B_2 and H_P are a fundamental set of directions, there are enough degrees of freedom to separate the effects of faults in thrust, elevator and airspeed sensor: this can be done by selecting the observer parameter R such that $RB_i = \mathbf{e}_i$, $i = 1, 2$ and $RH_P = \mathbf{e}_3$.*

V. Case study

Let us consider the case study of a small unmanned aircraft, the Aerosonde UAV (AAI Corporation, Textron Inc.). Initial conditions for the state variables have been chosen as follows:

$$\nu_0 = 22.9 \ m/s, \quad \alpha_0 = 0.1 \ rad, \quad q_0 = 0, \quad \theta_0 = 0.$$

Assuming the air pressure $\rho = 1.2682 \ Kg/m^3$, geometric and aerodynamical parameters for computing the linear longitudinal model of the aircraft are given in the following table [12]:

m	13.5 Kg		Z_ν	-0.5385 m/s^2
I_{xx}	0.8244 Kg/m^2		Z_α	-2.1277 s^{-1}
I_{yy}	1.135 Kg/m^2		Z_q	22.95 m/s
I_{zz}	1.759 Kg/m^2		M_ν	-0.1134 (m $\cdot$ s)$^{-1}$
I_{xz}	0.1204 Kg/m^2		M_α	-12.1204 s^{-2}
$\mathcal{S}$	0.55 m^2		M_q	-0.4602 s^{-1}
$\bar{c}$	0.1899 m		$X_{\delta_{th}}$	59.0570 s^{-1}
			X_{δ_e}	-0.4939 m/s^2
X_ν	-0.4365 s^{-1}		Z_{δ_e}	4.9230 m/s^2
X_α	-0.8802 m/s^2		$M_{\delta_{th}}$	0 (m $\cdot$ s)$^{-1}$
X_q	-2.3027 m/s		M_{δ_e}	-15.5248 s^{-2}

The aircraft attitude is supposed to be controlled by an autopilot, responsible to maintain the steady-state flight conditions in spite of wind disturbances: a state-feedback control loop has been implemented for this scope. The wind acceleration has been assumed to be bounded:

$$|\dot{\omega}_x| \leq 15m/s^2, \quad |\dot{\omega}_z| \leq 2m/s^2$$

Several scenarios have been analyzed, namely:

1) Thrust fault and vertical wind disturbance
2) Elevator fault and vertical wind disturbance
3) Thrust fault with noisy sensors
4) Thrust fault with model uncertainties
5) Airspeed sensor fault
6) Incremental and total icing

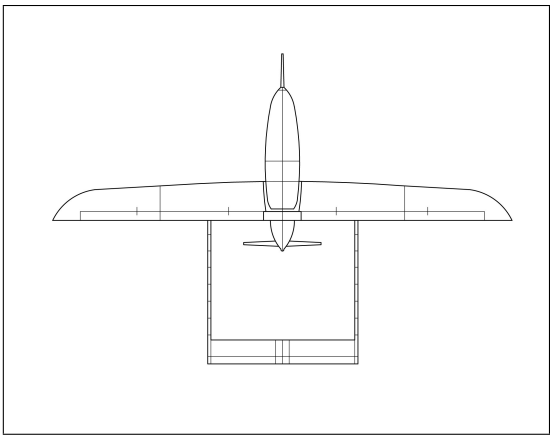

Fig. 3. Aerosonde UAV: top view

Scenario 1: The effective thrust input δ_{th} is supposed to be subject to a loss of efficiency with respect to its nominal value δ_{th}^*, i.e.

$$\delta_{th}(t) = \exp(-0.02t)\delta_{th}^*(t).$$

The residual evaluation is depicted in Figure 4. It can be easily verified that only the components along directions $\mathbf{e}_1$ and $\mathbf{e}_3$ are affected, that is $\epsilon(t) \in \mathcal{V}_{1,3}$. According to Decision Algorithm 1, the occurrence of a thrust failure together with the presence of a vertical wind disturbance can be correctly identified.

Scenario 2: In this second scenario the effective elevator deflection δ_e is supposed to be subject to a loss of efficiency with respect to its nominal value δ_e^*, i.e.

$$\delta_e(t) = \exp(-0.005t)\delta_e^*(t).$$

Figure 5 shows that the residual component along direction $\mathbf{e}_2$ is not interested by the fault: therefore we have $\epsilon(t) \in \mathcal{V}_{1,3}$, this addressing the fault isolation task. We notice that a fault in the elevator results in the instability of the component $\mathbf{e}_2$, corresponding to an uncontrolled deviation of the angle-of-attack.

Scenario 3: Let us consider the same framework analyzed in Scenario 1 and, in addition, let us suppose the measurements to be affected by noise. Referring to Figure 6, it can be easily verified that the presence of noisy observations does not influence the efficiency of the fault isolation scheme, in particular the condition $\epsilon(t) \in \mathcal{V}_{1,3}$ still holds.

Scenario 4: As further variation of Scenario 1, one can consider the case of model uncertainties. Figure 7 shows the residual evaluation when the system matrices are subject to bounded uncertainties

$$A + \Delta A, \quad B + \Delta B,$$

where $|\Delta A|$, $|\Delta B|$ are supposed to be 0.01% deviations from $|A|$ and $|B|$, respectively. The excitation of component $\mathbf{e}_2$ is negligible and not persistent; hence, up to a small tolerance factor, we still have $\epsilon(t) \in \mathcal{V}_{1,3}$.

Scenario 5: The case of airspeed sensor fault is addressed. The fault ξ is supposed to be proportional to the airspeed ν:

$$\xi = 0.1\exp(0.001t)|\nu|.$$

Referring to the construction given in Remark II.1, the following parameters have been considered:

$$\sigma_x = 1, \quad \sigma_z = 0.9,$$

this leading to the vector $P = [1\ 0.035\ 0\ 0]^T$. The coefficient of wind estimation error is assumed to be of the same order as σ_x, i.e. $c_\omega \simeq \sigma_x$; for sake of simplicity we set $c_\omega = 1$. The residual evaluation is illustrated in Figure 8: it is straightforward to verify that $\epsilon(t) \in \mathcal{V}_{1,2}$ and, according to Decision Algorithm 2, this provides the identification of a fault in the airspeed sensor.

Scenario 6: In this last scenario we analyze the effects of icing on the UAV dynamics. Two cases have been considered: incremental icing, with η slowly increasing from 0 to 0.1, and total icing with $\eta = 0.2$. The residual evaluation is shown in Figure 9 and Figure 10, respectively. In both cases, all residual components $\mathbf{e}_1, \mathbf{e}_2$ and $\mathbf{e}_3$ are permanently excited and this implies $\epsilon(t) \in \mathcal{V}_\sharp$: the icing detection condition in Decision Algorithm 1 and Decision Algorithm 2 is therefore fulfilled.

VI. Conclusions and future work

This paper is focused on designing an UIO-based scheme for icing detection in Unmanned Aerial Vehicles. Decision algorithms have been proposed in order to correctly identify possibly unexpected effects in the system dynamics: wind disturbances, actuator and sensor faults, icing. As a first step of a wide research project, in the present paper the aircraft longitudinal linearized model has been considered, and the icing effect has been modeled as a variation of the system matrices, depending on the icing severity parameter η.
The case study of icing detection for the Aerosonde UAV has been included as a validation of the proposed results.
Future investigations in this topic will be focused on:

- Extension of the previous results to the complete 9-DOF aircraft model, exploiting input redundancy and designing fault tolerant control reconfiguration schemes.
- Generalization of icing model by considering different effects on distinct aircraft surfaces, actuators and/or sensors.

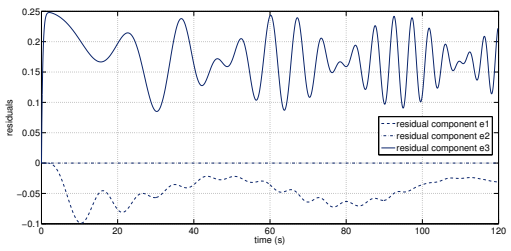

Fig. 4. Residual evaluation: vertical wind and thrust fault

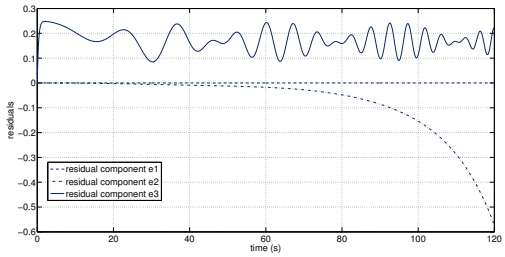

Fig. 5. Residual evaluation: vertical wind and elevator fault

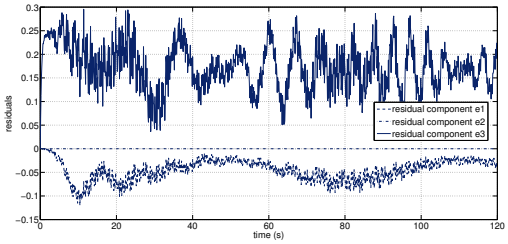

Fig. 6. Residual evaluation in the presence of noisy measurements: vertical wind and thrust fault

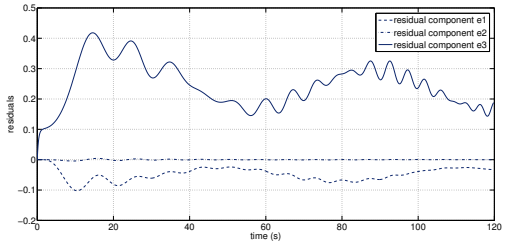

Fig. 7. Residual evaluation in the presence of model uncertainties: vertical wind and thrust fault

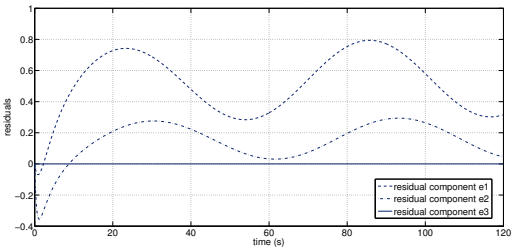

Fig. 8. Residual evaluation: airspeed sensor fault

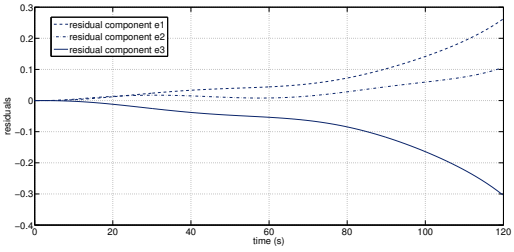

Fig. 9. Residual evaluation: incremental icing ($\eta \in [0, 0.1]$)

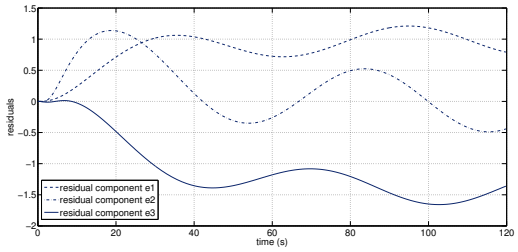

Fig. 10. Residual evaluation: total icing ($\eta = 0.2$)

REFERENCES

[1] Y. Zhang and J. Jiang, "Bibliographical review on reconfigurable fault tolerant control systems," *Ann. Rev. in Control*, vol. 32, pp. 229–252, 2008.

[2] R. W. Gent, N. P. Dart, and J. T. Cansdale, "Aircraft icing," *Phil. Trans. of the Royal Soc. of London. Series A: Mathematical, Physical and Engineering Sciences*, vol. 358, pp. 2873–2911, 2000.

[3] T. G. Myers and D. W. Hammond, "Ice and water film growth from incoming supercooled droplets," *Int. Journal of Heat and Mass Transfer*, vol. 42, pp. 2233–2242, 1999.

[4] M. B. Bragg, A. P. Broeren, and L. Blumenthal, "Iced-airfoil aerodynamics," *Progress in Aerospace Sciences*, pp. 323–362, 2005.

[5] S. Bone and M. Duff, "Carbon nanotubes to de-ice UAVs," *http://136.142.82.187/eng12/Author/data/2122.docx*, Technical report, 2012.

[6] T. Johansen and T. Fossen, "Control allocation: A survey," *Automatica*, vol. 49, pp. 1087–1103, 2013.

[7] A. Cristofaro and T. A. Johansen, "Fault-tolerant control allocation using unknown input observers," *Automatica*, in press, 2014, http://dx.doi.org/10.1016/j.automatica.2014.05.007.

[8] J. Tjònnås and T. Johansen, "Adaptive control allocation," *Automatica*, vol. 44, pp. 2754–2766, 2008.

[9] A. Casavola and E. Garone, "Fault-tolerant adaptive control allocation schemes for overactuated systems," *Int. J. Robust and Nonlinear Control*, vol. 20, pp. 1958–1980, 2010.

[10] H. Alwi and C. Edwards, "Sliding mode FTC with on-line control allocation," *Proc. 45th IEEE Conf. on Decision and Control*, pp. 5579–5584, 2006.

[11] M. Tousi and K. Khorasani, "Robust observer-based fault diagnosis for an unmanned aerial vehicle," in *Systems Conference (SysCon), 2011 IEEE International*, 2011, pp. 428–434.

[12] R. Beard and T. McLain, *Small unmanned aircrafts - Theory and practice*. Princeton University press, 2012.

[13] E. Lavretsky and K. A. Wise, *Robust adaptive control with aerospace applications*. London: Springer, 2013.

[14] S. Hansen and M. Blanke, "Diagnosis of airspeed measurement faults for unmanned aerial vehicles," *IEEE Transactions on Aerospace and Electronic Systems*, vol. 50, no. 1, pp. 224–239, 2014.

[15] G. Ducard, K. Rudin, S. Omari, and R. Siegwart, "Strategies for sensor-fault compensation on UAVs: review, discussions and additions," *European Control Conference 2014, Strasbourg (France)*, pp. 1963–1968, 2014.

[16] D. Houck and L. Atlas, "Air data sensor failure detection," in *Digital Avionics Systems Conference, 1998. Proceedings., 17th DASC. The AIAA/IEEE/SAE*, vol. D17, 1998, pp. 1–8.

[17] M. B. Bragg, T. Hutchinson, J. Merret, R. Oltman, and D. Pokhariyal, "Effect of ice accretion on aircraft flight dynamics," *Proc. 38th AIAA Aerospace Science Meeting and Exhibit*, 2000.

[18] J. Langelaan, N., Alley, and J. Neidhoefer, "Wind field estimation for small unmanned aerial vehicles," *Journal of Guidance, Control, and Dynamics*, vol. 34, no. 4, pp. 1016–1030, 2011.

[19] J. Chen, R. Patton, and H. Zhang, "Design of unknown input observers and robust detection filters," *Int. J. of Control*, vol. 63, pp. 85–105, 1996.